Proceedings of the Thirty-sixth (2026) International Ocean and Polar Engineering Conference www.isope.org
Orlando, Florida, USA, May 31-June 5, 2026

ISBN 978-1-880653-72-2; ISSN 1098-6189

Hydroelastic Response of a Trimaran in Waves Based on CFD-MBD Method

Zhihao Wang[1], Songtao Chen[2], Haotuo Qu[2], Yuji Miao[2], Jianhua Wang[1], Decheng Wan[1]*

[1] Computational Marine Hydrodynamics Lab (CMHL), School of Ocean and Civil Engineering,
Shanghai Jiao Tong University, Shanghai, China
[2] China Ship Scientific Research Center, Wuxi, China
[*]Corresponding Author

ABSTRACT

Trimarans have drawn attention due to the complexity of their structure. In this paper, a fully coupled fluid-structure interaction method is proposed to study trimaran hydroelastic responses. A two-way coupling method based on CFD-MBD (Computational Fluid Dynamics and Multi Body Dynamics) is constructed using open source software OpenFOAM and MBDyn. The flow field is solved using the RANS equations in OpenFOAM, while the structural dynamic responses are calculated using the beam model in MBDyn. The hydroelastic responses are analyzed. The longitudinal distribution trends of the shear force and VBM (vertical bending moment) show that the maximum force occurs in the bow and the maximum bending moment occurs in the middle of the ship. The port side and the starboard side of the connector have the same shear force and bending moment. The stern of the side hull receives higher shear force and bending moment than the bow of the side hull.

KEY WORDS: Ship hydroelasticity, Fluid-structure interactions, Two-way coupling Trimaran, CFD-MBD

INTRODUCTION

As an emerging high-performance vessel in recent years, trimarans have garnered attention from researchers worldwide due to their excellent seaworthiness and outstanding stability. However, their complex hull structure leads to intricate structural responses when subjected to wave loads. Consequently, studying the motion, impact, and structural response of trimarans during navigation has become essential.

The hydroelastic problem in ships is a typical fluid-structure interaction problem. Depending on the solution approach, computational methods for fluid-structure interaction studies can be categorized into two types: monolithic coupling (also known as direct coupling) and partitioned coupling (also known as iteration coupling). Based on the nature of the physical field coupling relationship, fluid-structure interaction analysis methods can be categorized into two types: one-way coupling methods and two-way coupling methods.

Dr. Paik (2009, 2010) developed a numerical prediction program for ship hydroelastic response based on unidirectional coupling theory using the team's internal solver CFDShip-Iowa. This program was validated against S-175 standard model test data. Dr. Seng (2012) and Dr. Oberhagemann (2012, 2016) independently developed ship rigid-body motion solver modules within the OpenFOAM framework based on Newton's second law. and an elastic deformation solver for hull beams based on the Timoshenko beam theory. They integrated these structural solvers with OpenFOAM's interDyMFoam solver to develop a two-way fluid-structure interaction solver for ship hydroelasticity. Wei et al. (2022a) developed a ship hydroelastic solver by integrating the open-source fluid solver OpenFOAM, the open-source structural solver CalculiX, and the open-source fluid-structure interaction interpolation library preCICE. They subsequently validated the solver by comparing its results with experimental data and numerical simulations from other researchers. Wei et al. (2022b) integrated the open-source fluid solver OpenFOAM with the open-source structural solver MBDyn. They further developed a data interface for fluid-structure interaction interpolation exchange and created a corresponding ship hydroelastic solver. The solver was validated using the S-175 container ship model. Building upon this foundation, Wei et al. applied the developed solver to address engineering challenges including: numerical prediction of hydroelastic responses following hull damage and water ingress (2023); investigation of hydroelastic responses for ultra-large floating structures considering mooring effects (2024a); and numerical prediction of hydroelastic responses for floating breakwaters with additional elastic baffles (2024b). Zhang et al. employed the OpenFOAM-MBDyn coupling method to solve and analyze the fluid-structure interaction hydroelastic problem of ultra-large container ships in waves （2025a） and the reliability of the coupled solution using the third-party wave generation software waves2Foam with OpenFOAM-MBDyn was verified (2025b).

Chen et al. (2019) develop an accurate and efficient method for evaluating the hydroelastic load and motion responses of high-speed trimarans, in oblique irregular waves. Liao et al. (2021) analyze the seakeeping and slamming behaviors of a trimaran in oblique regular waves using Computational Fluid Dynamics (CFD) and emphasizes that slamming in oblique waves is more practically significant because roll motion causes frequent emergence and water entry of side hulls, which is rare in head waves.

So far there has been little research on the hydroelasticity of trimaran especially with a structure of multi beam model. This paper focuses on the hydroelastic behavior of trimaran vessels in waves, employing the open-source software OpenFOAM-preCICE-MBDyn for fluid-structure interaction (FSI) coupling analysis to examine structural loads on the multi-body beam hull structure during wave exposure.

NUMERICAL METHOD

Coupling Method

In this study, a partitioned strong coupling strategy is adopted to investigate the hydroelastic responses of a trimaran. This approach effectively decouples the fluid and structural domains both physically and numerically, allowing for the utilization of specialized solvers for each physics field. The solvers are synchronized and connected via a coupling interface to exchange boundary data.

The numerical simulation platform comprises three core components:

Fluid Solver: The open-source Computational Fluid Dynamics(CFD) toolbox, OpenFOAM, is employed to solce the Unsteady Reynolds-Averaged Naiver-Stokes(URANS) equations, capturing hydrodynamic loads, free surface evolution, and flow field characteristics.

Structure Solver: The multi-body dynamics software, MBDyn, is utilized to resolve the equations of motion for the rigid-flexible coupled system. The ship hull is discretized into nonlinear beam elements, capable of simultaneously capturing large-amplitude rigid body motions (e.g., pitch, heave) and elastic deformations (e.g., springing, whipping).

Coupling Interface: The open-source library preCICE (Precise Code Interaction Coupling Environment) serves as the black-box coupling middleware. It manages data mapping between non-conformal meshes, time interpolation, and the acceleration of coupling convergence.

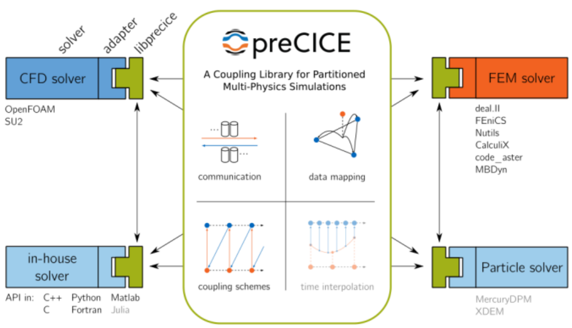

Fig. 1 Components of preCICE

Fluid Simulation Method

The fluid domain is discretized using the Finite Volume Method (FVM). Assuming an incompressible two-phase flow (air and water), the governing equations are the continuity equation and the momentum conservation equation:

$$\nabla \cdot \mathbf{U} = 0 \tag{1}$$

$$\frac{\partial(\rho \mathbf{U})}{\partial t} + \nabla \cdot (\rho \mathbf{U}\mathbf{U}) = -\nabla p + \nabla \cdot \boldsymbol{\tau} + \rho \mathbf{g} + \mathbf{F}_s \tag{2}$$

where $\mathbf{U}$ denotes the velocity vector, p is the pressure, ρ represents the mixture density, and $\boldsymbol{\tau}$ is the viscous stress tensor. The Volume of Fluid (VOF) method is implemented to capture the free surface interface by solving the transport equation for the phase fraction α .

To accommodate the motion and deformation of the hull boundary, the Arbitrary Lagrangian-Eulerian (ALE) method is applied. The motion of the fluid mesh satisfies the Geometric Conservation Law (GCL). The boundary condition at the fluid-structure interface Γ is governed by the kinematic continuity condition:

$$\mathbf{x}_{f,\Gamma}^{n+1} = \mathbf{x}_{s,\Gamma}^{n+1} \tag{3}$$

Structural Simulation Method

The structural response analysis is based on Multi-Body Dynamics (MBD) theory. In MBDyn, the hull is modeled as a system comprising rigid nodes and flexible elements (e.g., geometrically exact beams). The equations of motion are formulated as a set of differential-algebraic equations (DAEs), typically expressed in the form:

$$\mathbf{M}(\mathbf{q})\ddot{\mathbf{q}} + \mathbf{C}(\mathbf{q},\dot{\mathbf{q}})\dot{\mathbf{q}} + \mathbf{K}(\mathbf{q})\mathbf{q} = \mathbf{F}_{ext} + \mathbf{F}_{fluid} \tag{4}$$

where $\mathbf{q}$ is the generalized coordinate vector (including rigid body translations/rotations and elastic modal coordinates), and **M,C and K** represent the generalized mass, damping, and stiffness matrices, respectively. $\mathbf{F}_{fluid}$ denotes the hydrodynamic loads (pressure and shear stress) integrated from the fluid solver. This formulation allows for a unified solution of low-frequency rigid body motions and high-frequency hydroelastic vibrations.

SHIP MODEL AND SIMULATION CONDITIONS

Ship Model

The model selected in this paper is a trimaran benchmark. The length between perpendiculars is 5.49m. The main parameters of the model is

Table 1 Main parameters of the model

Parameters	Main hull	Side hull
Length between perpendiculars (Lpp)/m	5.49	1.87
Breadth/m	2.13	0.35
Draft/m	0.23	0.23
Displacement/kg	379.41	14.95

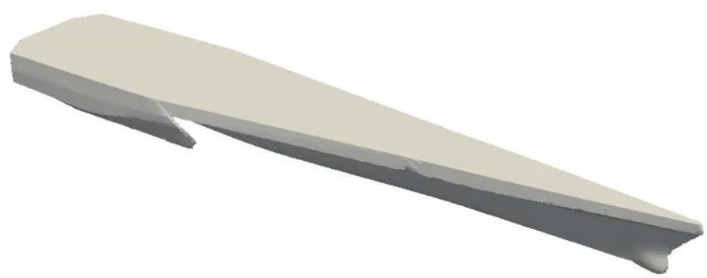

Fig. 2 Ship model

Hull Beam Model

In MBDyn, the hull beam is decomposed into several three-node beam models. The three-node beam element in MBDyn is implemented based on the finite volume method and the Geometrically Exact Beam Theory (GEBT), a theory for accurately modeling beams. It accounts for the beam's geometric nonlinearity and torsional stiffness, enabling the simulation of beam motion and deformation in three-dimensional space. This approach considers effects such as lateral bending, shear, and axial compression to more precisely simulate beam behavior. On each side is a three-node beam model. Each three-node beam includes three beam nodes and two interpolation points. Interpolation points are used to store bending moment and shear force information, while beam nodes are used to store displacement information.

In the ship's hull beams, each beam node is connected to a node fixed to the ground. Each node can be independently released with degrees of freedom, while adjacent nodes maintain relative degrees of freedom.
Unlike the single-beam model used for conventional ships, trimaran vessels employ a multi-beam model for structural modeling. This paper employs a four-beam model for structural modeling of the trimaran.

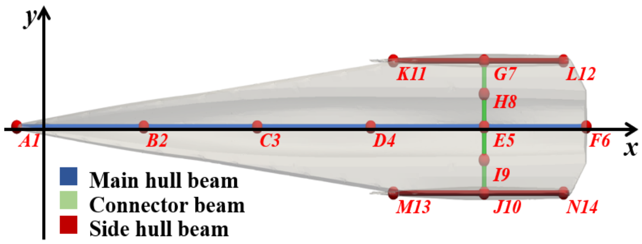

Fig. 3 Trimaran beam model

The four-beam model contains fourteen nodes as is shown in Fig. 3. In the hull beam nodes, the E5, G7, and J10 nodes employ fixed support conditions to satisfy actual physical constraints. The remaining nodes use free-free conditions. The structural loads of the wing section and main hull section are transmitted through the connecting bridge structure. Structural load information from the wing section is conveyed to the connecting bridge structure via G7 and J10; structural load information from the main hull section is conveyed to the connecting bridge structure via E5.

Computational Grid

The numerical modeling process comprises three distinct modeling components: the construction of the hull beam, the structural grid, and the fluid grid. The final solution involves beam deformation, but a structural mesh is required for the intermediate transition. Structural meshes are generated using the same method as fluid meshes, though they are coarser in resolution. The flow field loads are calculated by integrating the flow field mesh over the hull surface. The computed fluid loads are then mapped onto the structural surface mesh and further transferred to the hull beams via interpolation points.

After receiving the forces for the new time step, the structural field solves the structural dynamics equations of the beams to determine the structural deformation of the hull beams at that time step. Subsequently, based on the deformation quantities at a finite number of nodes on the hull beams, these values are interpolated and mapped to the deformation quantities at nodes in the hull surface structural mesh. This data is then transferred to the flow field mesh to obtain the total displacement at mesh nodes across different hull locations, thereby correspondingly modifying the coordinates of the mesh nodes at those positions.

In this numerical simulation, the computational domain is set as follows: $-1.0L_{PP} < X < 3.0L_{PP}, -1.0L_{PP} < Y < 1.0L_{PP}, -2.0L_{PP} < Z < 1.0L_{PP}$. A wave-making relaxation region of $0.5\,L_{PP}$ in length is provided at the inlet of the computational domain, and an extinction relaxation region of $1.0L_{PP}$ in length is provided at the outlet.
The computational domain is set as shown in Fig. 4. The red portion in the image represents the water phase, while the blue portion represents the atmosphere.

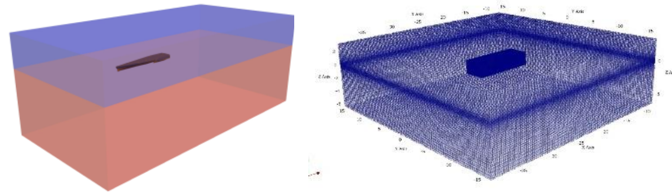

(a) computational domain (b) computational grid
Fig. 4 Computational domain and computational grid

Simulation Conditions

The responses of the ship under regular waves were calculated using elastic ship models. The amplitude of the wave is 0.05m, period is 1.85s, wavelength λ / L_{pp} is 1.1.

RESULT AND DISCUSSION

The wavefront conditions under this operating condition are shown in Fig. 5.

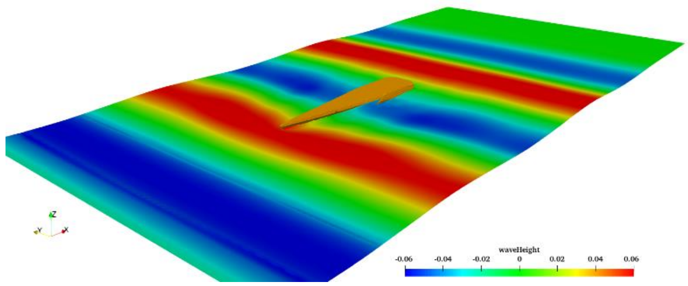

Fig. 5 Wave elevation

The pressure distribution on the hull surface and bottom at the current time step is shown in Fig. 6 (a) and (b).

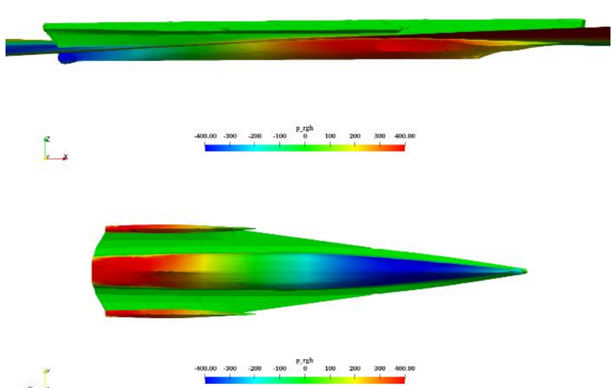

Fig. 6 Pressure distribution along ship

The linear displacement at the midship node is used as the time history of heave, while the angular displacement at the bow and stern nodes is used as the time history of pitch. The resulting time history curves are shown in Fig. 7 and Fig. 8. Time* is a dimensionless parameter representing time, calculated by dividing time t by the wave period. Heave*is calculated by dividing heave by the wave amplitude.

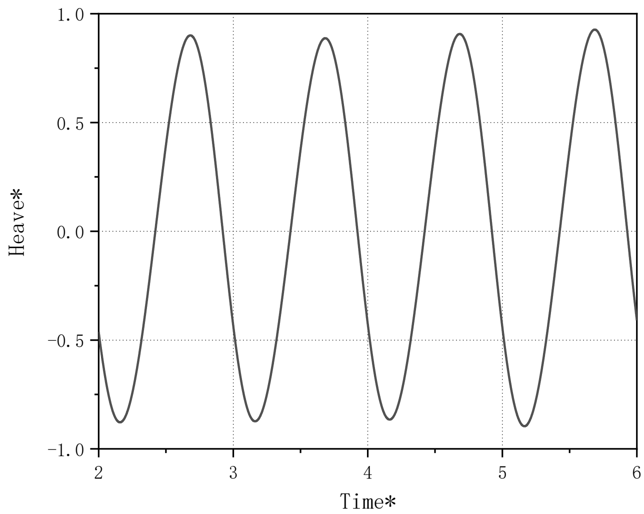

Fig. 7 Time history of heave motion

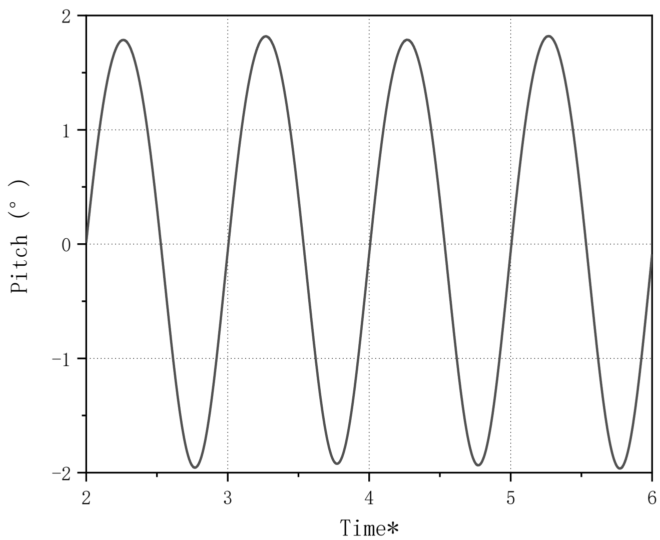

Fig. 8 Time history of pitch motion

The time history curves indicate that the ship's vertical roll amplitude is approximately 0.4m, while the pitch amplitude is around 2.0°. Both the roll and pitch time history curves align with the wave height time history. The peak and trough values and amplitudes of vertical roll and pitch are summarized in the table below.

Table 2 Ship Motion Statistics

Parameters	Wave elevation	Heave (m)	Pitch (°)
Peak	0.051	0.046	1.81
Trough	-0.050	-0.045	-1.93
Amplitude	0.051	0.046	1.87

By extracting structural load data from different nodes along the ship's beams, load time history curves can be plotted at various positions along the ship's length, as shown in the figure below. Node numbers are shown in Fig. 3.

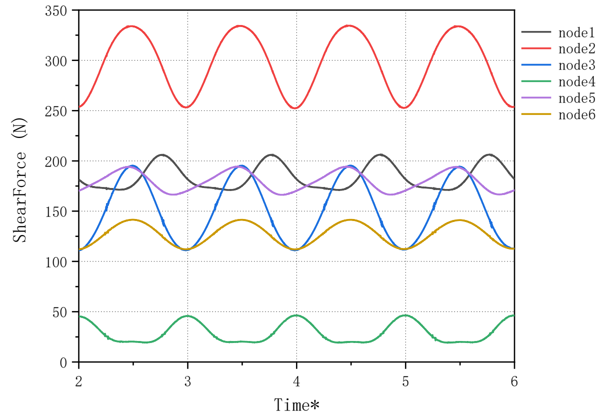

Fig. 9 Shear stress distribution along the main hull at different nodes in the longitudinal direction

Observing the time history curve reveals that the shear force time history follows the same trend as the wave height time history. Along the ship's length, the shear force exhibits an initial increase followed by a decrease. The distribution of structural shear forces between the hull connection bridge and the plate sections is shown in Fig. 10 and Fig. 11.

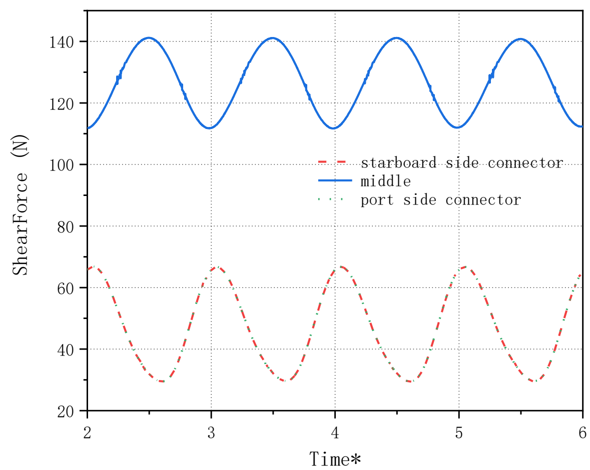

Fig. 10 Shear distribution at the connection bridge

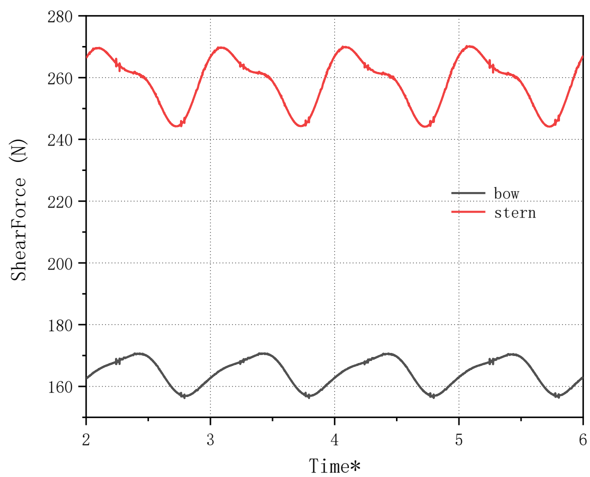

Fig. 11 Shear distribution at the side hull

As shown in Fig. 10, the shear distribution at the nodes on both sides of the connecting bridge is identical, with shear amplitudes significantly

lower than those at the connection points with the main hull. Under wave-riding conditions, the shear forces on the port and starboard hull sections are identical. Therefore, when plotting the history using only the port hull section's shear force.
Extract the shear peak values, valley values, and amplitudes at different nodes to plot the shear amplitude distribution along the ship's length. As shown in the figure below.

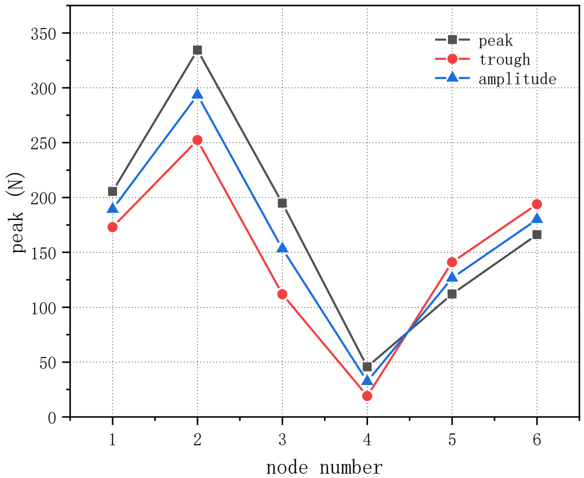

Fig. 12 Shear distribution along the hull

As shown in the figure, the shear force along the ship's length exhibits a trend of first decreasing and then increasing. The shear force is minimal at the midship section, while it is greater on both sides. The extracted shear values are plotted as shown in Table 3.

Table 3 Shear Amplitude of Main Hull Beam

Node number	Peak(N)	Trough(N)	Amplitude(N)
1	205.55	172.96	189.255
2	334.36	252.34	293.35
3	194.82	111.8	153.31
4	45.67	19.05	32.36
5	112.1	141	126.55
6	166.2	193.9	180.05

The shear amplitude values for the connector and side hulls are shown in Table 4.

Table 4 Shear amplitude of the connector and the side hulls

Node position	Peak(N)	Trough(N)	Amplitude(N)
Middle connector	111.7	141.2	126.4
Starboard side connector	66.7	29.5	48.1
Port side connector	65.8	30.2	48.0
Side hull bow	268.0	244.5	256.2
Side hull stern	156.1	169.2	162.7

The bending moment data extracted from different node positions of the vessel is plotted as a time-history curve as shown in Fig. 13.

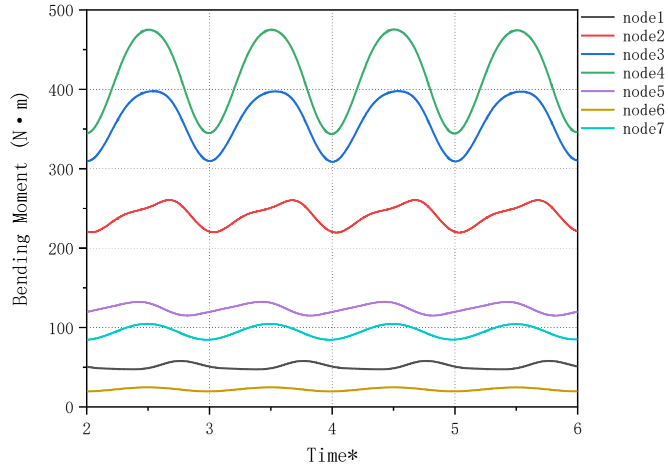

Fig. 13 bending moments distribution along the main hull beam

The bending moment time history distribution of the main hull beam shows that the bending moment increases along the ship's length before decreasing. The maximum bending moment occurs at node 4.

The bending moment data of the connector and side hulls is shown in Fig. 14 and Fig. 15.

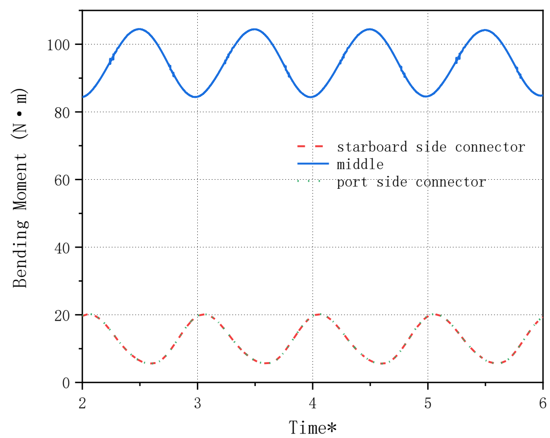

Fig. 14 Bending moment of connector beam

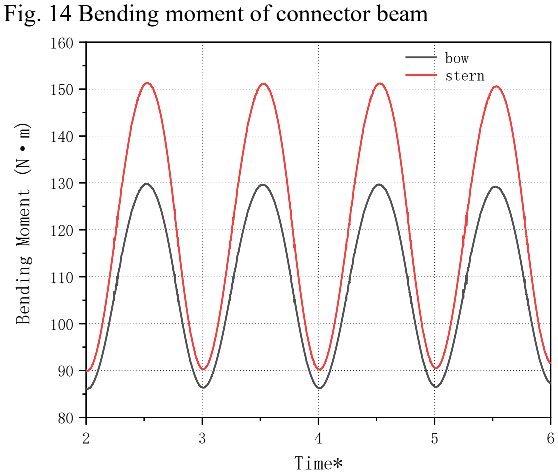

Fig. 15 Bending moment of side hull

The bending moment magnitude at the intermediate node of the connecting bridge is greater than that at the nodes on either side. The bending moment magnitudes at the bow and stern of the side hull are similar but in opposite directions.
Extract the peak, valley, and amplitude values of each hull beam section and plot the amplitude distribution curve along the ship's length.

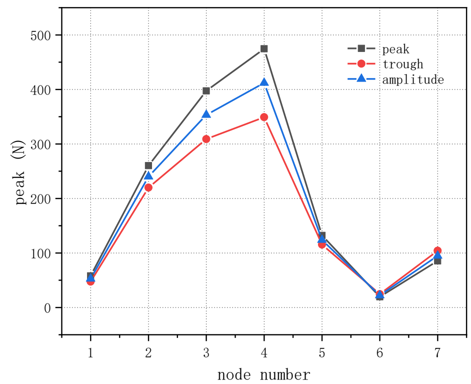

Fig. 16 Bending moment along hull

Extract the amplitude values from each node and compile them into a table, as shown below.

Table 5 Bending moment amplitude of main hull beam

Node number	Peak(N)	Trough(N)	Amplitude(N)
1	57.98	47.44	52.71
2	260.25	219.96	240.105
3	397.39	308.98	353.185
4	474.58	349.19	411.885
5	132.24	115.3	123.77
6	-19.58	-24.59	22.085
7	-85.53	-104.2	94.865

The table also shows that the amplitude increases along the ship's length before decreasing, with the maximum bending moment occurring at the midship position.

Table 6 Bending monemt amplitude of the connector and the side hulls

Node position	Peak(N)	Trough(N)	Amplitude(N)
Middle connector	-84.39	-104.4	94.395
Starboard side connector	-5.71	-20.12	12.915
Port side connector	-5.71	-20.12	12.915
Side hull bow	-86.28	-129.4	107.84
Side hull stern	151.13	90.57	120.85

CONCLUSIONS

This paper investigates the elastic response of trimarans in waves. Numerical simulations of the structural response of trimarans in waves are conducted using CFD-MBD two way coupling method. Under wave-riding conditions, the structural responses of the left and right sections of the trimaran are essentially identical. The distribution of shear forces and bending moments in the hull of a trimaran under wave loading is consistent with that of a conventional monohull vessel. Shear forces reach their maximum values at the bow and stern, while bending moments peak at the midship section. The shear forces and bending moments at the left and right nodes of the connecting bridge near the side hull sections are both smaller than those at the nodes in the middle section of the connecting bridge. For the hull section, both the shear force and bending moment at the bow exhibit characteristics opposite to those at the stern.
Subsequent work will increase the number of hull beam nodes to more accurately simulate structural loads at various locations throughout the hull. Additionally, numerical simulation analysis will be conducted on the structural loads experienced by trimarans at high speeds under different wave height conditions. This analysis will examine bow impact loads, impact loads at the connecting bridges, and the RAO curve of the vessel's motion.

ACKNOWLEDGEMENTS

This work was supported by the Stabilization Support Research Project (WDZC70202030205), to which the authors are most grateful.

REFERENCES

CHEN Z Y, GUI H, DONG P, et al (2019). Numerical and experimental analysis of hydroelastic responses of a high-speed trimaran in oblique irregular waves. International Journal of Naval Architecture and Ocean Engineering. 11(1), 409-421.
LIAO X Y, CHEN Z Y, GUI H, et al (2021). CFD prediction of ship seakeeping and slamming behaviors of a trimaran in oblique regular waves. Journal of Marine Science and Engineering. 9(10), 1151.
OBERHAGEMANN J, SHIGUNOV V, MOCTAR O (2012). Application of CFD in Long-Term Extreme Value Analyses of Wave Loads. *Ship Technology Research*. 59(3), 4-12.
PAIK K J (2010). Simulation of fluid-structure interaction for surface ships with linear/nonlinear deformations. *Iowa: The University of Iowa*, 8-24.
PAIK K J, CARRICA P M, LEE D, et al (2009). Strongly coupled fluid–structure interaction method for structural loads on surface ships. *Ocean Engineering*. 36, 1346-1357.
SENG S (2012). Slamming and whipping analysis of ships. *Copenhagen: Technical University of Denmark.*
WEI Y J, INCECIK A, TEZDOGAN T (2022a). A fully coupled CFD-DMB approach on the ship hydroelasticity of a containership in extreme wave conditions. Journal of Marine Science and Engineering, 10, 1778.
WEI Y J, TEZDOGAN T (2022b). A fluid-structure interaction model on the hydroelastic analysis of a container ship using preCICE. *Proc 41st International Conference on Ocean, Offshore and Arctic Engineering*, Hamburg, Germany, 85925.
WEI Y J, INCECIK A, TEZDOGAN T (2023). A hydroelasticity analysis of a damaged ship based on a two-way coupled CFD-DMB method. *Ocean Engineering*. 274, 114075.
WEI Y J, YU S R, Jin P, et al (2024a). Coupled analysis between catenary mooring and VLFS with structural hydroelasticity in waves. *Marine Structures*. 93, 103516.
WEI Y J, YU S R, LI X, et al (2024b). Hydrodynamic analysis of a heave-hinge wave energy converter combined with a floating breakwater. *Ocean Engineering*, 293, 116618.
ZHANG W J, WANG J H, GUO H, et al (2025a). Numerical investigations of ship hydroelasticity of a 20,000 TEU containership based on CFD-MBD method. *Ocean Engineering*, 317, 120061.
ZHANG W J, ZHUANG Y, WAN D C, et al (2025b). Hydroelastic performance of an ultra-large containership in irregular and freak waves. *Physics of Fluids*, 37(2), 027190.